iScience

CellPress
OPEN ACCESS

Article

Diurnal *in vivo* xylem sap glucose and sucrose monitoring using implantable organic electrochemical transistor sensors

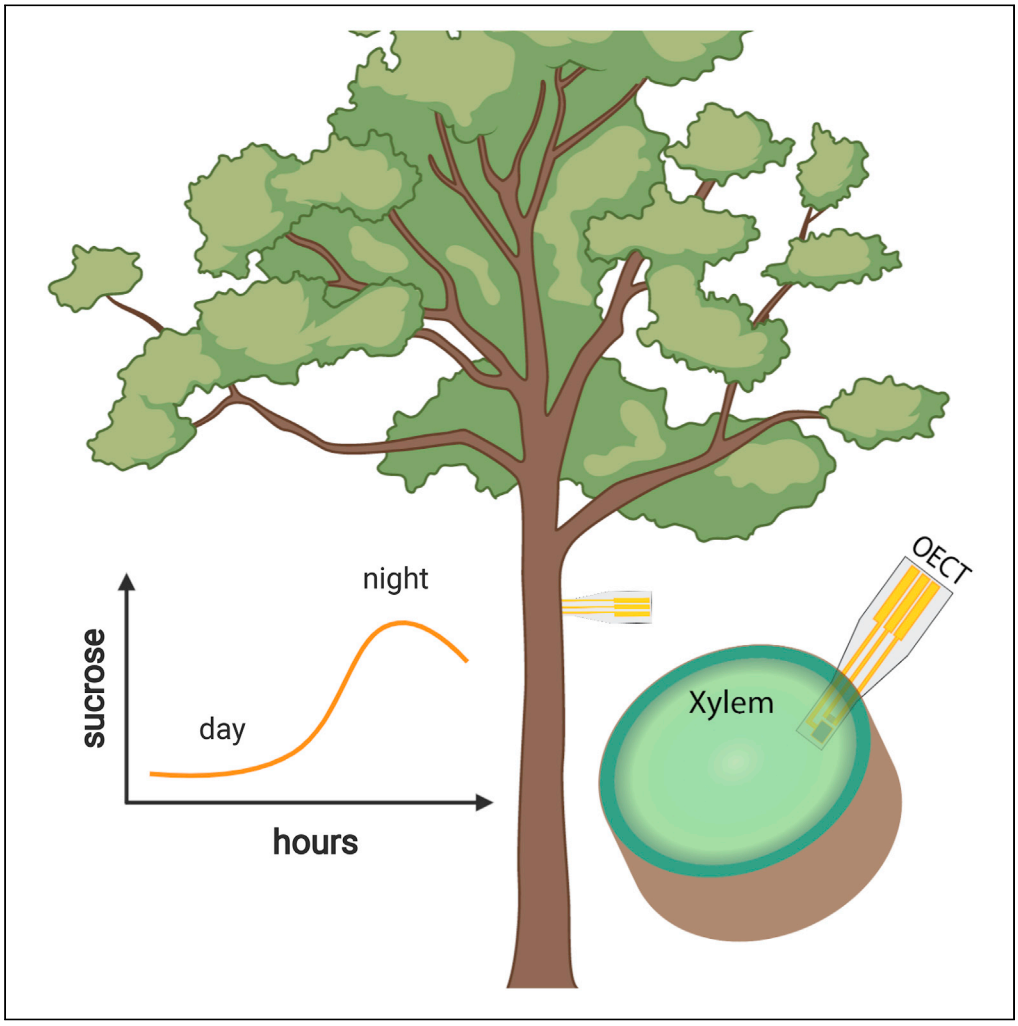

Chiara Diacci, Tayebeh Abedi, Jee Woong Lee, ..., Daniel T. Simon, Totte Niittylä, Eleni Stavrinidou

totte.niittyla@slu.se (T.N.)
eleni.stavrinidou@liu.se (E.S.)

Highlights

In vivo, real-time monitoring of sugars fluctuations in trees with OECTs for 48hr

OECTs reveal previously uncharacterized diurnal sucrose fluctuations in aspen

Multienzyme functionalization of OECT for detection of sucrose

Operation of sensors with low-cost portable unit

Diacci et al., iScience 24, 101966
January 22, 2021
https://doi.org/10.1016/j.isci.2020.101966

iScience

CellPress
OPEN ACCESS

Article

Diurnal *in vivo* xylem sap glucose and sucrose monitoring using implantable organic electrochemical transistor sensors

Chiara Diacci,[1,2] Tayebeh Abedi,[3] Jee Woong Lee,[1,4] Erik O. Gabrielsson,[1] Magnus Berggren,[1,4] Daniel T. Simon,[1] Totte Niittylä,[3,*] and Eleni Stavrinidou[1,4,5,*]

Summary

Bioelectronic devices that convert biochemical signals to electronic readout enable biosensing with high spatiotemporal resolution. These technologies have been primarily applied in biomedicine while in plants sensing is mainly based on invasive methods that require tissue sampling, hindering in-vivo detection and having poor spatiotemporal resolution. Here, we developed enzymatic biosensors based on organic electrochemical transistors (OECTs) for in-vivo and real-time monitoring of sugar fluctuations in the vascular tissue of trees. The glucose and sucrose OECT-biosensors were implanted into the vascular tissue of trees and were operated through a low-cost portable unit for 48hr. Our work consists a proof-of-concept study where implantable OECT-biosensors not only allow real-time monitoring of metabolites in plants but also reveal new insights into diurnal sugar homeostasis. We anticipate that this work will contribute to establishing bioelectronic technologies as powerful minimally invasive tools in plant science, agriculture and forestry.

Introduction

Bioelectronics enable electronic interfacing with the biological world as means for monitoring or stimulating biological processes. The bioelectronics field is highly driven by applications in biomedicine, specifically finding new solutions for diagnosis and therapy (Berggren and Richter-Dahlfors, 2007; Zeglio et al., 2019). Organic electronic devices can be advantageous when applied in the biological milieu since organic electronic materials support sufficient electronic and ionic transport (Paulsen et al., 2020), in a highly coupled manner, and thus enable efficient signal transduction. While the majority of efforts lie within the animal kingdom, applying bioelectronics to other biological organisms has emerged with successful demonstrations of sensing and actuation in bacteria (He et al., 2012; Pitsalidis et al., 2018; Zajdel et al., 2018; Demuru et al., 2019; Di Lauro et al., 2020) and plants (Stavrinidou et al., 2015, 2017; Coppedè et al., 2017; Poxson et al., 2017; Bernacka-Wojcik et al., 2019; Janni et al., 2019; Kim et al., 2019; Vurro et al., 2019; Diacci et al., 2020). Recently, we presented an implantable organic electronic ion pump for *in vivo* delivery of abscisic acid, one of the main hormones involved in plant stress responses (Bernacka-Wojcik et al., 2019), and subsequently the electronic control of physiology in intact plants. Others demonstrated conformable electrodes based on conducting polymers that were directly printed on plant leaves for long term bioimpedance monitoring (Kim et al., 2019). In another work, a yarn-based organic electrochemical transistor (OECT) has been used for electrolyte monitoring in tomato plants in physiological conditions (Coppedè et al., 2017), while in following works, the same concept was used to monitor drought stress (Janni et al., 2019) or changes in vapor pressure deficit (Vurro et al., 2019). Our group coupled an OECT directly with isolated chloroplasts to monitor in real-time the glucose export from the plant organelles with unprecedented time resolution (Diacci et al., 2020). The OECT is a three terminal device where a gate electrode modulates the current, via reduction-oxidation switching of a conducting polymer-based channel (Nilsson et al., 2002; Rivnay et al., 2018). The OECTs operate in aqueous environments and when the gate electrode is functionalized with an enzyme the OECT is converted to an enzymatic biosensor (Tang et al., 2011). When the analyte is present in the solution, an electrochemical reaction takes place at the gate, which becomes amplified through the modulation of the channel current. Signal amplification of the OECTs is important particularly for miniaturized devices where high signal to noise ratio is challenging. Although OECTs have received a lot of attention as amplification biosensors, their application in complex

[1]Laboratory of Organic Electronics, Department of Science and Technology, Linköping University, 601 74 Norrköping, Sweden

[2]Dipartimento di Scienze della Vita, Università di Modena e Reggio Emilia, Via Campi 103, 41125 Modena, Italy

[3]Umeå Plant Science Centre, Department of Forest Genetics and Plant Physiology, Swedish University of Agricultural Sciences, 90183 Umea, Sweden

[4]Wallenberg Wood Science Center, Linköping University, 601 74 Norrköping, Sweden

[5]Lead Contact

*Correspondence: totte.niittyla@slu.se (T.N.), eleni.stavrinidou@liu.se (E.S.)

https://doi.org/10.1016/j.isci.2020.101966

biological environments has been very limited. So far, most of the enzymatic OECT sensors have been validated in test solutions for the detection of metabolites and neurotransmitters (Shim et al., 2009; Kergoat et al., 2014; Liao et al., 2014; Berto et al., 2018; Pappa et al., 2018). Few demonstrations have been reported where glucose is monitored from natural samples such as sweat (Scheiblin et al., 2015) saliva (Liao et al., 2015; Pappa et al., 2016), or cell media (Curto et al., 2017; Strakosas et al., 2017) and one example focused on epidermal patches for on-body detection (Parlak et al., 2018). Until now, there is no demonstration of an implantable OECT enzymatic sensor for monitoring an analyte directly within the *in vivo* environment.

Sugars are produced by photosynthesis and play a central role in plant growth and development. Several of the primary sugar metabolic pathways, responsible for carbon allocation in plants, are relatively well described. One of the current challenges in the field is to understand how the metabolic pathways of sugar metabolism are regulated, and how changes in sugar flux or concentration are adjusted. In order to address these questions, methods allowing for spatial and temporal real-time quantification of sugar levels are needed. The development of Förster resonance energy transfer (FRET)–based nanosensors for sugars was the first step toward *in vivo* measurements of sugar pools (Deuschle et al., 2006; Chaudhuri et al., 2011). Genetically encoded FRET sensors enable the analysis of steady-state concentration of sugar and dynamic changes in living tissue with high temporal and even subcellular resolution. However, the use of FRET sugar sensors is limited to cells and tissues, which can be monitored using a microscope. Cells buried deep in tissues, as is the case of vascular system, for example, are not accessible. Therefore, sugar analysis in plants, is usually performed by invasive methods that have poor spatial and temporal resolution and lead to disposal of the organism or tissue after sampling. Furthermore, sample analysis requires extraction/processing followed by sugar level determination based on enzymatic assays (Graf et al., 2010), mass spectrometry (Jorge et al., 2016) or high-performance liquid chromatography (Mayrhofer et al., 2004). All of these methods have high accuracy and low detection limit, but do not enable *in vivo* real time sugar level monitoring and therefore impede kinetic studies and analysis of biologically relevant events within the living plant.

In several tree species, including the model tree aspen, sucrose is the predominant form of transported carbon (Rennie and Turgeon, 2009). Sucrose is primarily transported in the phloem to different parts of the plant, but sucrose is also transported within the xylem transpiration stream (Heizmann et al., 2001; Mayrhofer et al., 2004). It was estimated that 9–28% of the carbon delivered to leaves in 3-month-old *Populus* trees over a diurnal cycle was derived from sugars transported in the transpiration stream (Mayrhofer et al., 2004). Several tree species also use the xylem pathway to transport sugars during flowering and bud flush in the spring (Sauter and Ambrosius, 1986). Xylem sap composition is typically analyzed from exudate secreted from a cut stem or leaf petiole. Sometimes, root pressure is sufficient to push out the xylem sap from the cut, but often a pressure chamber is required to squeeze out the sap and there is always a concern that xylem sap may mix with phloem sap or other cell contents at the cut surface. Furthermore, these invasive methods disrupt the transpiration stream, and do not allow monitoring of the sap composition over time. In this work, we overcome the above limitations by developing implantable glucose and sucrose OECT-based sensors that enable *in vivo* real time monitoring in plants (Figure 1). As a demonstration of the proof-of-concept and the kind of biological insights that this technology enables, we observed previously uncharacterized diurnal changes in sucrose levels in the xylem sap of greenhouse-grown hybrid aspen (*Populus tremula* x *tremuloides*).

Results and discussion

OECT-based sugar sensors

The OECT-based glucose and sucrose sensors were fabricated on a 125-μm-thick polyethylene naphthalate (PEN) substrate using standard microfabrication techniques as described in the Transparent Methods section. Ti/Au is used for source, drain, gate electrodes, and for wiring while the channel is based on the conducting polymer poly(3,4-ethyl-enedioxythiophene):poly(styrenesulfonate) (PEDOT:PSS). The gate electrode is coated with a PEDOT:PSS thin film in order to increase its capacitance for efficient modulation of the channel conductance and is then further functionalized with enzymes and PtNPs. The PtNPs were electrodeposited on the gate while the enzymes were immobilized with the help of a chitosan matrix that is drop-casted onto the gate.

The PEDOT:PSS-based OECT operates in the depletion mode with the channel initially at the high conductance state. When a positive bias is applied at the gate, cations from the electrolyte will penetrate into the channel, compensating the PSS polymer dopants resulting in PEDOT de-doping and a decrease in the

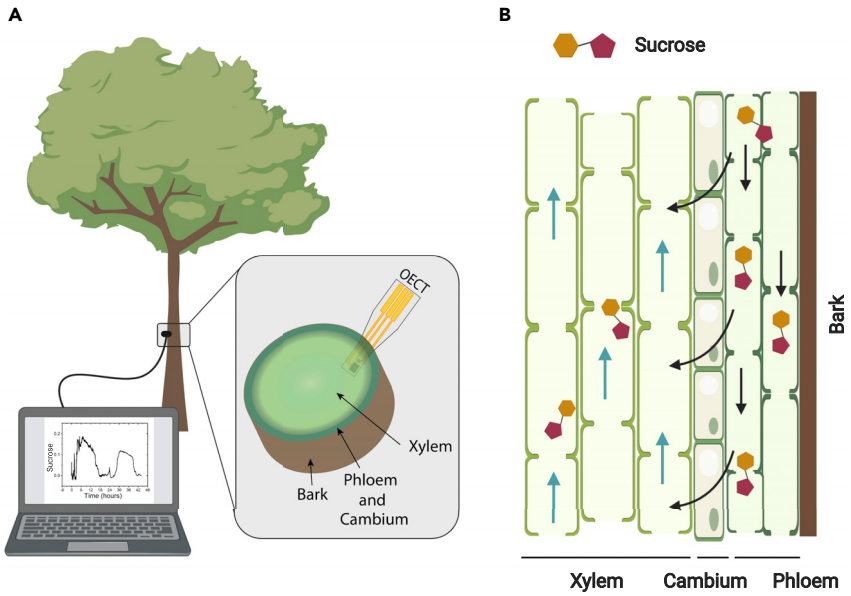

Figure 1. *In vivo* sugar monitoring in trees with an OECT-based biosensor

(A) Illustration of the experimental setup. In the inset, the OECT biosensor is placed within the tissue of interest, the mature xylem of the tree.

(B) Illustration of the vascular tissue of trees. Phloem is the main tissue responsible for sucrose transport. Sucrose is unloaded from phloem into xylem (black arrow) and then being transported via the transpiration stream (blue arrows).

channel current (Khodagholy et al., 2013). When the analyte is present in the solution an enzymatic reaction will take place at the gate that will result in the generation of H_2O_2. The H_2O_2 will then be oxidized on the PtNPs on the gate, which is associated with a transfer of electrons that change the effective gate potential and consequently induce a further decrease in the channel current (Bernards et al., 2008) (Figure 2A). Typical transfer curve and transconductance of the OECT are shown in Figure 2B. The transconductance is considered the figure of merit of OECT sensor devices as describes the change in the drain current over the change in gate potential, $g_m = \Delta I_D/\Delta V_G$. Therefore, operation of the device at the high transconductance regime will result in small changes in the gate potential to induce large changes in the channel current. The analytes possible to detect by the enzymatic electrochemical sensors are limited by the availability of enzymes that can take part in redox reactions. Glucose oxidase is an oxido-reductase enzyme that catalyzes the oxidation of β-D-glucose to hydrogen peroxide and D-glucose1,5-lactone. Sucrose on the other hand does not have a corresponding oxidoreductase enzyme. In order to detect sucrose enzymatically, we overcame this limitation by incorporating successfully three enzymes within the chitosan matrix enabling a cascade of reactions to take place in a confined space. First, invertase hydrolyzes sucrose into fructose and α-D-glucose, mutarotase then catalyzes the conversion of α-D-glucose into β-D-glucose and finally β-D-glucose reacts with the glucose oxidase enzyme, Figure 2A.

The performance and sensitivity range of the OECT-based glucose and sucrose sensors were assessed by monitoring the relative change of the channel current in solutions containing increasing concentration of sugars. To achieve high sensitivity, we operated the transistor at voltages across the gate, V_{GS} = +0.5 V and channel, V_{DS} = −0.4 V (source grounded), where the OECT has high transconductance, and thus exhibiting high amplification of the sensor signal. In order to compare the response of different devices and extract the characteristic calibration curve of the sensor we calculated the normalized drain current response of the device for each analyte concentration ($\Delta I/I = -(I_{[M]}-I_0)/I_0$), where $I_{[M]}$ is the drain current at concentration M and I_0 is the base drain current. In Figure 2C, we show the calibration curves of the sucrose and glucose sensors represented as the mean of the response of 8 and 5 different devices, respectively. We observe that the sensors have similar, close to identical, characteristics with a dynamic range within 100 μM - 1 mM, as a result of the same concentration of glucose oxidase enzyme in the sucrose and glucose sensor. Furthermore, our biofunctionalization strategy allows us to tune the sensitivity and dynamic response of the sensor by changing the concentrations of the enzymes within the chitosan matrix. As shown in Figure S1, the sensor becomes sensitive to higher concentrations of sucrose when we reduce the

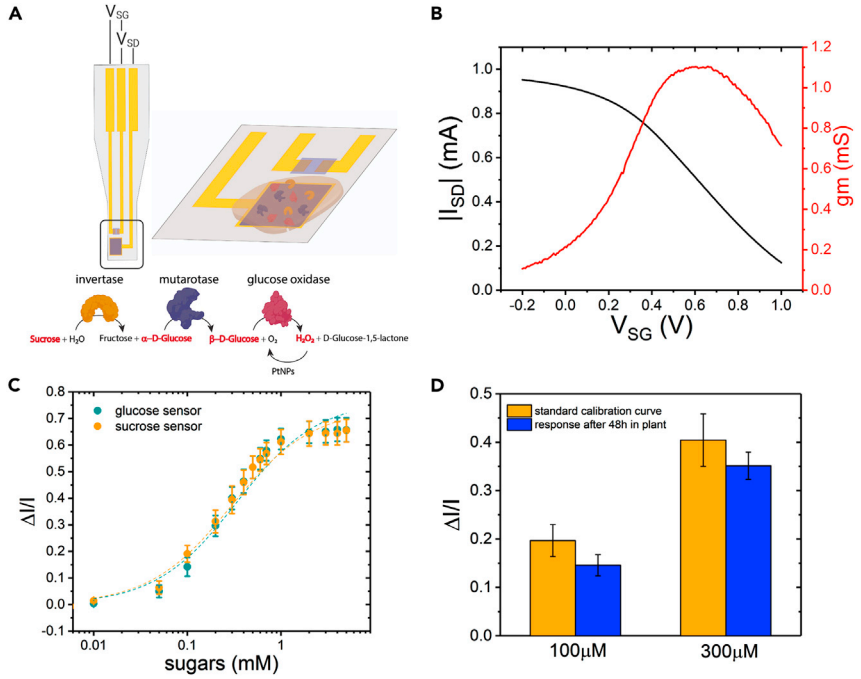

Figure 2. OECT-based sucrose and glucose sensors

(A) Schematic of the OECT-based sucrose sensor. Gate (area = 300 μm * 300 μm) is functionalized with three enzymes in order for sucrose to be converted to H_2O_2 that can then be oxidized at the PtNPs that are on the gate electrode.

(B) Typical transfer curve and transconductance of OECT device after functionalization with PtNPs for V_{SD} = −0.4V and V_{SG} from −0.2V to 1V.

(C) Sucrose sensor (orange) and glucose sensor (cyan) calibration curve in PBS buffer. Dashed lines represent fit to the sigmoidal function. Error bars represent the standard error, n = 8 devices for sucrose sensor and n = 5 devices for glucose sensor.

(D) Sucrose sensor response after 48hr of insertion in the tree for 100 μM and 300μM sucrose solutions (blue error bars represent the standard error for n = 3). In orange, the sucrose sensor calibration curve is shown for comparison. T test showed no statistical significance ($p > 0.05$) on the response of the sensors before and after 48hr implantation.

enzymes concentrations. Additionally, we tested the sensitivity of the sucrose sensor to glucose. Indeed, we observe that the sucrose sensor is sensitive to glucose as it is expected, Figure S2. Therefore, for the *in vivo* detection of glucose and sucrose both independent sensors were used simultaneously. Finally, we evaluated the stability of the sensor in the complex biochemical environment of the plant. Sucrose sensor devices (n = 3) were implanted in the bark of hybrid aspen trees for 48hr and after being removed from the tree their response to 100μM and 300μM of sucrose test solutions was assessed as shown in Figure 2D. We observe a small decrease in the sensor response in comparison with the standard calibration curve of the sucrose sensors but the difference is not statistically significant.

Device integration and portable measurement setup

Next, we proceed to develop a portable OECT measurement unit set-up based on a low-cost Arduino platform that allow us to perform the sensing experiment in the growth environment of plants. In this case, the measurements were performed inside the greenhouse while these devices can be also operated in growth chambers or even in field conditions (Figures 3A and 3B). As the platform uses uni-polar analog-to-digital and digital-to-analog converters it was operated using a common drain configuration (i.e. drain was grounded) in order to avoid negative voltages (Figure 3C). Two identical but separate circuits were used to source gate and source voltages (V_{GD}^{in} and V_{SD}^{in}) and simultaneously measure gate and source currents (I_G and I_S).

Each circuit was composed of a voltage output (V_{GD}^{out} or V_{SD}^{out}) connected to one end of a precision resistor ($R_G$or R_S). The other end of the resistor was connected to a voltage input (V_{GD}^{in} or V_{SD}^{in}) and to the gate or source terminals. The drain terminal was connected to the ground of the microcontroller. Externally the gate, source and drain terminals were connected to the OECT using a ZIF connector and a ribbon cable

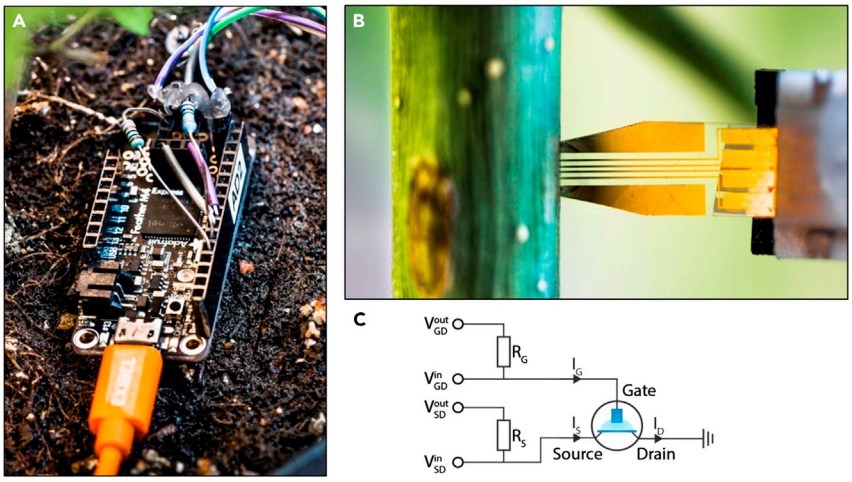

Figure 3. Portable measurement setup

(A) Portable Arduino measurement unit.

(B) OECT connected through ZIF connector and inserted in hybrid aspen tree stem.

(C) Schematic of the Arduino measurement unit circuit. V_{GD} and V_{DS} is related to V_{GS} and V_{DS} through $V_{GD} = V_{GS} - V_{DS}$ and $V_{SD} = - V_{DS}$.

(Figure 3B). Two proportional-integral-derivative (PID) controllers were used to control the voltages applied to the gate and source terminals of the OECT. Upon application of V^{out}, the voltage loss over R reduces the voltage at the gate/source terminal. The PID compensates for this by measuring V^{in} and modulating V^{out} so that V^{in} matches the desired gate/source voltage. The voltage over R, obtained from the difference between $V^{out}$and V^{in}, was used to calculate I_G and $I_S$through Ohm's law using the known value of R.

OECT insertion and wounding response

In order to perform meaningful *in vivo* measurements with the OECT sensors it is important to minimize wound responses caused by the sensor insertion. Wounding responses may interfere with the measurements by altering the physiological processes of interest. Therefore, we first evaluated the response to the insertion of the sensor. We used hybrid aspen *(Populus tremula x tremuloides)* as our model system and mature xylem as the tissue of interest. The OECT design was optimized for this specific biological system. The sensors were fabricated on a flexible and thin PEN substrate with a thickness of 125 μm to ensure enough mechanical stability that enables easy insertion while decreasing the footprint to minimize invasiveness. Moreover the device was encapsulated with an SU-8 layer in order to ensure that only the active area of the transistor, gate and channel are exposed to the plant environment. The length of the implanted part of the sensor was chosen to be 3 mm to guarantee that the active sensor site reaches the mature xylem tissue and transpiration stream and the width chosen to 1 mm. An initial incision with a scalpel was performed to allow sensor insertion to the correct site at 3 mm depth from the epidermis (Figure 4A). This ensured that the sensor gate and channel are located within the mature xylem and are in contact with the transpiration stream. Any local wound response is unlikely to have a substantial effect on the composition of the xylem sap flowing past the sensor, but tissue repair responses may eventually lead to the isolation of the sensor from the transpiration stream. Therefore, wound responses due to the OECT insertion was analyzed over a time course of 1, 2, and 5 days using an optical light microscope. The visual changes in the insertion site were recorded using a camera and analyzed in more detail by preparing 60 μm thick cross sections across the insertion site using a vibratome (Figure 4B). The cross sections were stained with Toluidine Blue O solution to aid the visualization of the cell walls and any tissue level changes. These assays established that a local wound response due to OECT implantation was evident after 48 hr and obvious after 5 days when also a cork tissue formation was observed (Figure 4B). Hence, the following *in vivo* sugar measurements were limited to the first 48 hr following sensor insertion.

Real-time sugar monitoring via implantable OECTs

Sucrose and glucose OECT-based sensors were implanted into the mature xylem of greenhouse grown 8-week-old hybrid aspen trees, and operated at constant gate voltage of V_{GD} = +0.5 V and constant

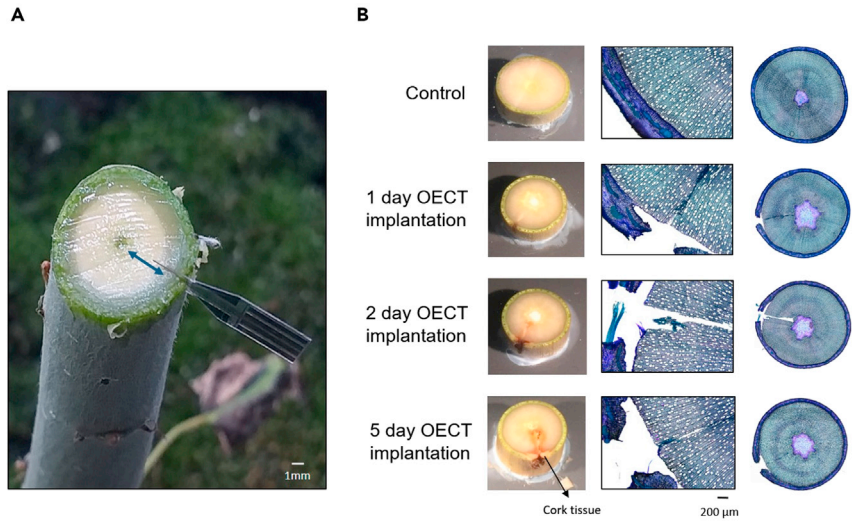

Figure 4. Insertion site and wounding effect

(A) OECT inserted in the hybrid aspen tree stem, showing the active area of the device in the xylem tissue (blue arrow indicates the mature xylem), scale bar 1 mm.

(B) Optical microscopy images of stem cross-sections displaying the OECT wounding effect. Control and hybrid aspen tree response after 1, 2, and 5 days of insertion. Scale bar 200 µm.

source-drain voltage of V_{DS} = −0.4 V for 24 hr or 48 hr. Prior to the insertion in the trees, the sensors were treated with oxygen plasma to induce hydrophilicity and to improve the device performance within the xylem tissue (Figure S3). As a control, a device without any included enzyme(s) but with the PtNPs and chitosan matrix was inserted in the same region as the sensor devices. The control device allowed evaluation of any changes in the device response that were not caused from the presence of sugars. Interestingly, the sucrose sensor revealed a variation of the current between day-time and night-time, establishing that sucrose concentration in the xylem sap increases during darkness and decreases at the onset of the light period (Figures 5A and S4). To our knowledge, this is the first time that such diurnal fluctuation in sucrose concertation is observed in xylem sap. At the same time, glucose and control devices did not display any variation between day and night, indicating that glucose homeostasis is not affected by the sucrose changes (Figures 5A and S4). We always observed the same trend in increase of sucrose during the dark period, but the relative magnitude of the changes between different experiments within the same tree or different trees varied. The differences in relative magnitude may be explained by subtle internal and environmental differences, which are known to influence sucrose pools in plants (Farrar et al., 2000). The average change of the normalized response from day-time to night-time for the sucrose sensors is equal to $(I_{nigh}\text{-}I_{day})/I_{day}$ = 0.24 ± 0.1, n = 11), while in the control and glucose sensors there were no significant changes in the current (Figure 5B). We chose to treat our data only qualitatively and not to attempt to quantify the sucrose levels within the xylem due to the uncertainty of the concentration of sucrose in xylem prior insertion of the sensor as will be described below.

In order to compare the OECT findings with conventional methods, we analyzed day and night samples of xylem sap from aspen trees that were collected using the classical stem cutting and sap bleeding method (Alexou and Peuke, 2013). This is a highly invasive method where the tree stem is cut, the phloem is mechanically removed and the xylem sap is collected as it bleads out from the stem (Figure S5). The collected samples are then analyzed using an enzymatic assay (Stitt et al., 1989). The ex vivo analysis also showed an increase in xylem sap sucrose levels at night (Tables S1 and S2). However, unlike the in vivo measurements with the OECT sensors also glucose levels increased during night (Tables S1 and S2). We suspect that the glucose increase is due to the disruptive nature of the stem cutting and sap bleeding. With this method, pith cells are injured; therefore they are contributing to the collected liquid. Additionally, invertase enzymes, that are known to be induced by wounding (Roitsch and González, 2004), can catalyze sucrose cleavage to glucose and fructose. In support of this hypothesis, fructose levels increased similarly to glucose in the xylem sap collected from the cut stems (Tables S1 and S2). The ex vivo analysis limitations and uncertainties highlight the importance of developing minimally invasive in vivo methods for monitoring

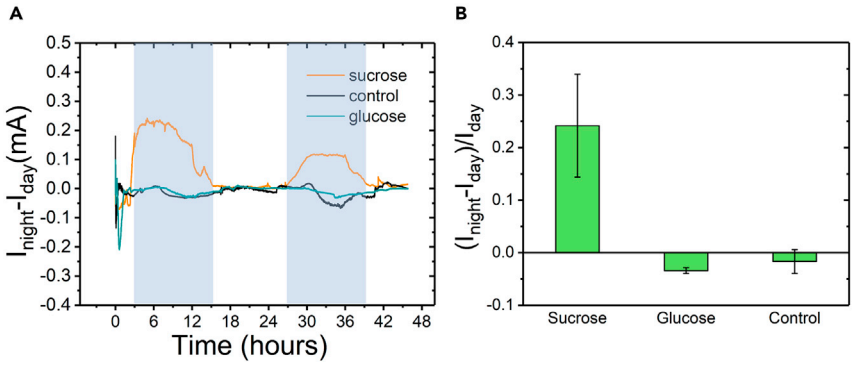

Figure 5. *In vivo*, real-time monitoring of sucrose and glucose in mature xylem of hybrid aspen

(A) Real time response of sucrose sensor (average for four experiments (orange)), glucose sensor (cyan) and control device (black) for 48hr in xylem tissue. Dark areas correspond to night-time and bright areas to day-time.

(B) Averaged normalized response of the sensors devices during nigh-time. I_{night} and I_{day} values were taken in the middle of the measured time for night and day respectively. Error bars represent the standard errors, sucrose sensors n = 11, glucose sensors n = 3, control devices n = 9.

sugars variations in plants and show how the OECT technology can overcome some of these limitations. Although we could attempt to quantify sucrose concentration changes based on the OECTs sensors response and taking as initial sucrose concertation the daytime value as determined from the ex vivo analysis, we avoided to do so considering all the uncertainties involved with the ex vivo analysis as described above. This then points out to the need of developing an internal reference system in the OECT that will enable us to treat the data quantitively as well, something that will be the focus of a future work.

Xylem sap transport of sugars has been reported for several tree species, including birch, willow, sugar maple, and *Populus* (Heizmann et al., 2001; Mayrhofer et al., 2004; Furukawa et al., 2011; Mahboubi and Niittylä, 2018). Changes in xylem sap sugar content are often associated with the spring time initiation of growth and flowering in temperate region species, illustrating the importance of the xylem sap sugar transport pathway for the seasonal growth of trees (Furukawa et al., 2011). Our experiments were conducted under controlled greenhouse conditions in fast-growing young aspen trees, which are not mobilizing long-term stores of carbon. The diurnal fluctuation in xylem sap sucrose levels that we observe with the OECT sensors is therefore likely to be associated with diurnal physiological and metabolic processes such as diurnal growth rate variation and starch degradation at night.

Diurnal xylem processes in trees have been observed for developing wood cell wall biosynthesis in young hybrid aspen trees (Mahboubi et al., 2015), and turgor pressure-driven diurnal changes in the stem diameter in *Cryptomeria japonica* (Hosoo et al., 2003). In the latter case, the stem diameter increased during the night and decreased during the day likely due to diurnal changes in water transpiration. Night time transpiration occurs in trees albeit at a lower level compared to day time (Daley and Phillips, 2006). However, since the OECT measurements showed that xylem sap glucose levels did not change, the sucrose change may be related to sucrose transport and/or storage rather than to sucrose cleavage, or a reduction in the xylem sap transport rate. We hypothesize that the diurnal changes in the xylem sap sucrose may be relevant for carbon allocation and as a diurnal cue at whole tree level. This example illustrates that the OECT sensor technology can provide new insights to carbon allocation and sugar metabolism in trees that cannot be obtained using classic xylem sap sampling methods.

Conclusions

In this work, we developed implantable OECT-based enzymatic biosensors that can operate in the complex *in vivo* environment for 48hr and in real-time monitor sugar variations in the vascular tissue of trees. We extended the range of analytes that can be detected enzymatically with an OECT by developing a biofunctionalization strategy that allows multiple enzymes to be immobilized in the same device and catalyze a chain reaction. Furthermore, we designed a cheap Arduino-based source-measure unit that allows the operation of the device in the growth environment of plants and showcase its potential for application in field conditions. One of the main limitations of our technology is that we can make only qualitative

observations as quantification is hindered by the unknown initial concertation of the analyte in the *in vivo* environment. Nevertheless, relative changes in biology are very important, and we report for the first time that sucrose in mature xylem shows a diurnal dependence indicating that sucrose transport in the xylem is correlated to metabolic or physiological processes. The principle of OECT technology can be applied to assess many metabolites, as well as, the effect of developmental and environmental cues, or abiotic and biotic stresses on the metabolites levels. The sensors are an example of non-invasive dynamic monitoring technology, which will contribute to a better understanding of tree growth dynamics. The technology may also find applications in related areas such as the study of xylem sap feeding insect behavior. Since the operation of the sensors does not depend on genetic modification, they can be readily applied in agriculture and forestry without ethical or societal restrictions. Although OECT technology development is highly driven by biomedical applications, our work demonstrates the usefulness and applicability of bioelectronic technologies in plants for elucidating fundamental questions that currently cannot be answered with the conventional methods and tools.

Limitations of the study

In this work, we reported OECT enzymatic biosensors for in vivo, real-time monitoring of sucrose and glucose variations in the xylem vascular tissue of hybrid aspen trees. Currently, our technology can be used only for qualitative observations as quantification is hindered by the unknown initial concertation of the analyte in the in vivo environment. Although relative changes in biology are important, quantifying the concertation of sugars will provide additional insight on the sugars transport. Furthermore, the wounding assay revealed that the plant is creating cork tissue after five days of implantation at the insertion point of the sensor which could result in isolating the sensors from the xylem and therefore limiting the duration of in vivo monitoring. Future work will focus on engineering further the sensor design to first enable quantitative in vivo sensing and secondly to minimizing cork tissue formation for extending the duration of real-time monitoring to several days.

Resource availability

Lead contact

Further information and requests for resources and materials should be directed to and will be fulfilled by the lead contact, Dr. Eleni Stavrinidou (eleni.stavrinidou@liu.se)

Materials availability

This study did not generate new unique reagents.

Data and code availability

Source data for the figures published in this the paper are available per request.

Methods

All methods can be found in the accompanying Transparent Methods supplemental file.

Supplemental information

Supplemental Information can be found online at https://doi.org/10.1016/j.isci.2020.101966.

Acknowledgments

The authors wish to thank Benoit Piro from Paris-Diderot University, Xenofon Strakosas and Per Jansson from Linköping University for fruitful discussions for the sensors design. Special thanks to Thor Balkhed, Linköping University for the photographs of Figures 3A and 3B. Funding was provided by the European Union's Horizon 2020 research and innovation program under grant agreement No 800926 (FET-OPEN-HyPhOE), the Swedish Foundation for Strategic Research (SSF), the Knut and Alice Wallenberg Foundation, the Wallenberg Wood Science Center, Vetenskapsrådet (VR), and the Swedish Government Strategic Research Area in Materials Science on Functional Materials at Linköping University (Faculty Grant SFO-Mat-LiU No. 2009-00971). This work was also supported by the Umea Plant Science Center, Berzelii Centre for Forest Biotechnology funded by VINNOVA. Additional funding was provided by a Marie Sklodowska Curie Individual Fellowship (MSCA-IFEF-ST, Trans-Plant, 702641) to ES and by an ERC-Advanced Grant to MB. Figures were created with BioRender.com.

Author contributions

E.S. and T.N. conceived and designed the project, C.D. fabricated and characterized the OECT-sensors and performed all in vivo experiments with the help of T.A. and J.L., T.A. performed the wounding assay and the ex vivo xylem sap collection and analysis, C.D. and T.A. analyzed data; E.G. developed the portable measurement platform; C.D., T.A., E.G., T.N. and E.S. wrote the initial draft and final manuscript with input from all the authors; E.S. and T.N. supervised the project.

Declaration of interests

The authors declare no competing interests.

Received: September 21, 2020
Revised: December 4, 2020
Accepted: December 15, 2020
Published: January 22, 2021

References

Alexou, M., and Peuke, A.D. (2013). Chapter 13 methods for xylem sap collection. Plant Mineral. Nutrients *953*, 195–207.

Berggren, M., and Richter-Dahlfors, A. (2007). Organic bioelectronics. Adv. Mater. *19*, 3201–3213.

Bernacka-Wojcik, I., Huerta, M., Tybrandt, K., Karady, M., Mulla, M.Y., Poxson, D.J., Gabrielsson, E.O., Ljung, K., Simon, D.T., Berggren, M., and Stavrinidou, E. (2019). Implantable organic electronic ion pump enables ABA hormone delivery for control of stomata in an intact tobacco plant. Small *15*, 1–9.

Bernards, D.A., Macaya, D.J., Nikolou, M., DeFranco, J.A., Takamatsu, S., and Malliaras, G.G. (2008). Enzymatic sensing with organic electrochemical transistors. J. Mater. Chem. *18*, 116–120.

Berto, M., Diacci, C., Theuer, L., Di Lauro, M., Simon, D.T., Berggren, M., Biscarini, F., Beni, V., and Bortolotti, C.A. (2018). Label free urea biosensor based on organic electrochemical transistors. Flexible and Printed Electronics, *3* (IOP Publishing), p. 24001.

Chaudhuri, B., Hörmann, F., and Frommer, W.B. (2011). Dynamic imaging of glucose flux impedance using FRET sensors in wild-type Arabidopsis plants. J. Exp. Bot. *62*, 2411–2417.

Coppedè, N., Janni, M., Bettelli, M., Maida, C.L., Gentile, F., Villani, M., Ruotolo, R., Iannotta, S., Marmiroli, N., Marmiroli, M., and Zappettini, A. (2017). An in vivo biosensing, biomimetic electrochemical transistor with applications in plant science and precision farming. Sci. Rep. *7*, 1–9.

Curto, V.F., Marchiori, B., Hama, A., Pappa, A.-M., Ferro, M.P., Braendlein, M., Rivnay, J., Fiocchi, M., Malliaras, G.G., Ramuz, M., and Owens, R.M. (2017). Organic transistor platform with integrated microfluidics for in-line multi-parametric in vitro cell monitoring. Microsyst. Nanoeng. *3*, 1–12.

Daley, M.J., and Phillips, N.G. (2006). Interspecific variation in nighttime transpiration and stomatal conductance in a mixed New England deciduous forest. Tree Physiol. *26*, 411–419.

Demuru, S. *et al.* (2019) 'Flexible Organic Electrochemical Transistor with Functionalized Inkjet-Printed Gold Gate for Bacteria Sensing', 2019 20th International Conference on Solid-State Sensors, Actuators and Microsystems and Eurosensors XXXIII, TRANSDUCERS 2019 and EUROSENSORS XXXIII. IEEE, 1(June), pp. 2519–2522.not available in PubMed,Crossref

Deuschle, K., Chaudhuri, B., Okumoto, S., Lager, I., Lalonde, S., and Frommer, W.B. (2006). Rapid metabolism of glucose detected with FRET glucose nanosensors in epidermal cells and intact roots of Arabidopsis RNA-silencing mutants. Plant Cell *18*, 2314–2325.

Di Lauro, M., la Gatta, S., Bortolotti, C.A., Beni, V., Parkula, V., Drakopoulou, S., Giordani, M., Berto, M., Milano, F., Cramer, T., et al. (2020). A bacterial photosynthetic enzymatic unit modulating organic transistors with light. Adv. Electron. Mater. *6*, 1–5.

Diacci, C., Lee, J.W., Janson, P., Dufil, G., Mehes, G., Berggren, M., Simon, D.T., and Stavrinidou, E. (2020). Real-time monitoring of glucose export from isolated chloroplasts using an organic electrochemical transistor. Adv. Mater. Tech. *5*, 1–6, 1900262.

Farrar, J., Pollock, C., and Gallagher, J. (2000). Sucrose and the integration of metabolism in vascular plants. Plant Sci. *154*, 1–11.

Furukawa, J., Abe, Y., Mizuno, H., Matsuki, K., Sagawa, K., Kojima, M., Sakakibara, H., Iwai, H., and Satoh, S. (2011). Seasonal fluctuation of organic and inorganic components in xylem sap of Populus nigra. Plant Root *5*, 56–62.

Graf, A., Schlereth, A., Stitt, M., and Smith, A.M. (2010). Circadian control of carbohydrate availability for growth in Arabidopsis plants at night. Proc. Natl. Acad. Sci. U S A *107*, 9458–9463.

He, R.-X., Zhang, M., Tan, F., Leung, P.H.M., Zhao, X.-Z., Chan, H.L.W., Yang, M., and Yan, F. (2012). Detection of bacteria with organic electrochemical transistors. J. Mater. Chem. *22*, 22072–22076.

Heizmann, U., Kreuzwieser, J., Schnitzler, J.-P., Brüggemann, N., and Rennenberg, H. (2001). Assimilate transport in the xylem sap of pedunculate oak (Quercus robur) saplings. Plant Biol. *3*, 132–138.

Hosoo, Y., Yoshida, M., Imai, T., and Okuyama, T. (2003). Diurnal differences in the innermost surface of the S2 layer in differentiating tracheids of Cryptomeria japonica corresponding to a light-dark cycle. Holzforschung *57*, 567–573.

Janni, M., Coppede, N., Bettelli, M., Briglia, N., Petrozza, A., Summerer, S., Vurro, F., Danzi, D., Cellini, F., Marmiroli, N., et al. (2019). In vivo phenotyping for the early detection of drought stress in tomato. Plant Phenomics *2019*, 1–10.

Jorge, T.F., Mata, A.T., and António, C. (2016). Mass spectrometry as a quantitative tool in plant metabolomics. Philos. Trans. A. Math. Phys. Eng. Sci. *374*, 20150370, Philosophical Transactions of the Royal Society A: Mathematical, Physical and Engineering Sciences.

Kergoat, L., Piro, B., Simon, D.T., Pham, M.C., Noël, V., and Berggren, M. (2014). Detection of glutamate and acetylcholine with organic electrochemical transistors based on conducting polymer/platinum nanoparticle composites. Adv. Mater. Weinheim *26*, 5658–5664.

Khodagholy, D., Rivnay, J., Sessolo, M., Gurfinkel, M., Leleux, P., Jimison, L.H., Stavrinidou, E., Herve, T., Sanaur, S., Owens, R.M., and Malliaras, G.G. (2013). High transconductance organic electrochemical transistors. Nat. Commun. *4*, 1–6.

Kim, J.J., Allison, L.K., and Andrew, T.L. (2019). Vapor-printed polymer electrodes for long-term, on-demand health monitoring. Sci. Adv. *5*, eaaw0463.

Liao, C., Zhang, M., Niu, L., Zheng, Z., and Yan, F. (2014). Organic electrochemical transistors with graphene-modified gate electrodes for highly sensitive and selective dopamine sensors. J. Mater. Chem. B *2*, 191–200.

Liao, C., Mak, C., Zhang, M., Chan, H.L., and Yan, F. (2015). Flexible organic electrochemical transistors for highly selective enzyme biosensors and used for saliva testing. Adv. Mater. Weinheim *27*, 676–681.

Mahboubi, A., Linden, P., Hedenström, M., Moritz, T., and Niittylä, T. (2015). 13C tracking

after 13CO2 supply revealed diurnal patterns of wood formation in aspen. Plant Physiol. *168*, 478–489.

Mahboubi, A., and Niittylä, T. (2018). Sucrose transport and carbon fluxes during wood formation. Physiol. Plant *164*, 67–81.

Mayrhofer, S., Heizmann, U., Magel, E., Eiblmeier, M., Müller, A., Rennenberg, H., Hampp, R., Schnitzler, J.P., and Kreuzwieser, J. (2004). Carbon balance in leaves of young poplar trees. Plant Biol. (Stuttg) *6*, 730–739.

Nilsson, D., Chen, M., Kugler, T., Remonen, T., Armgarth, M., and Berggren, M. (2002). Bi-stable and dynamic current modulation in electrochemical organic transistors. Adv. Mater. *14*, 51–54.

Pappa, A.M., Curto, V.F., Braendlein, M., Strakosas, X., Donahue, M.J., Fiocchi, M., Malliaras, G.G., and Owens, R.M. (2016). Organic transistor arrays integrated with finger-powered microfluidics for multianalyte saliva testing. Adv. Healthc. Mater. *5*, 2295–2302.

Pappa, A.M., Ohayon, D., Giovannitti, A., Maria, I.P., Savva, A., Uguz, I., Rivnay, J., McCulloch, I., Owens, R.M., and Inal, S. (2018). Direct metabolite detection with an n-type accumulation mode organic electrochemical transistor. Sci. Adv. *4*, 1–8.

Parlak, O., Keene, S.T., Marais, A., Curto, V.F., and Salleo, A. (2018). Molecularly selective nanoporous membrane-based wearable organic electrochemical device for noninvasive cortisol sensing. Sci. Adv. *4*, eaar2904.

Paulsen, B.D., Tybrandt, K., Stavrinidou, E., and Rivnay, J. (2020). Organic mixed ionic–electronic conductors. Nat. Mater. *19*, 13–26.

Pitsalidis, C., Pappa, A.M., Porel, M., Artim, C.M., Faria, G.C., Duong, D.D., Alabi, C.A., Daniel, S., Salleo, A., and Owens, R.M. (2018). Biomimetic electronic devices for measuring bacterial membrane disruption. Adv. Mater. *30*, 1–8.

Poxson, D.J., Karady, M., Gabrielsson, R., Alkattan, A.Y., Gustavsson, A., Doyle, S.M., Robert, S., Ljung, K., Grebe, M., Simon, D.T., and Berggren, M. (2017). Regulating plant physiology with organic electronics. Proc. Natl. Acad. Sci. U S A *114*, 4597–4602.

Rennie, E.A., and Turgeon, R. (2009). A comprehensive picture of phloem loading strategies. Proc. Natl. Acad. Sci. U S A *106*, 14162–14167.

Rivnay, J., Inal, S., Salleo, A., Owens, R.M., Berggren, M., and Malliaras, G.G. (2018). Organic electrochemical transistors. Nat. Rev. Mater. *3*, 1–14, 17086.

Roitsch, T., and González, M.C. (2004). Function and regulation of plant invertases: sweet sensations. Trends Plant Sci. *9*, 606–613.

Sauter, J.J., and Ambrosius, T. (1986). Changes in the partitioning of carbohydrates in the wood during bud break in betula pendula roth. J. Plant Physiol. *124*, 31–43.

Scheiblin, G., Aliane, A., Strakosas, X., Curto, V.F., Coppard, R., Marchand, G., Owens, R.M., Mailley, P., and Malliaras, G.G. (2015). Screen-printed organic electrochemical transistors for metabolite sensing. MRS Commun. *5*, 507–511.

Shim, N.Y., Bernards, D.A., Macaya, D.J., Defranco, J.A., Nikolou, M., Owens, R.M., and Malliaras, G.G. (2009). All-plastic electrochemical transistor for glucose sensing using a ferrocene mediator. Sensors (Basel) *9*, 9896–9902.

Stavrinidou, E., Gabrielsson, R., Gomez, E., Crispin, X., Nilsson, O., Simon, D.T., and Berggren, M. (2015). Electronic plants. Sci. Adv. *1*, e1501136.

Stavrinidou, E., Gabrielsson, R., Nilsson, K.P., Singh, S.K., Franco-Gonzalez, J.F., Volkov, A.V., Jonsson, M.P., Grimoldi, A., Elgland, M., Zozoulenko, I.V., et al. (2017). In vivo polymerization and manufacturing of wires and supercapacitors in plants. Proc. Natl. Acad. Sci. U S A *114*, 2807–2812.

Stitt, M., Lilley, R.Mc., Gerhardt, R., Heldt, H.W., et al. (1989). [32] Metabolite levels in specific cells and subcellular compartments of plant leaves. In Biomembranes Part U: Cellular and Subcellular Transport: Eukaryotic (Nonepithelial) Cells (Academic Press), pp. 518–552.

Strakosas, X., Huerta, M., Donahue, M.J., Hama, A., Pappa, A.M., Ferro, M., Ramuz, M., Rivnay, J., and Owens, R.M. (2017). Catalytically enhanced organic transistors for in vitro toxicology monitoring through hydrogel entrapment of enzymes. J. Appl. Polym. Sci. *134*, 1–7.

Tang, H., Yan, F., Lin, P., Xu, J., and Chan, H.L.W. (2011). Highly sensitive glucose biosensors based on organic electrochemical transistors using platinum gate electrodes modified with enzyme and nanomaterials. Adv. Funct. Mater. *21*, 2264–2272.

Vurro, F., Janni, M., Coppede, N., Gentile, F., Manfredi, R., Bettelli, M., and Zappettini, A. (2019). Development of an in vivo sensor to monitor the effects of vapour pressure deficit (VPD) changes to improve water productivity in agriculture. Sensors (Switzerland) *19*, 4667.

Zajdel, T.J., Baruch, M., Méhes, G., Stavrinidou, E., Berggren, M., Maharbiz, M.M., Simon, D.T., and Ajo-Franklin, C.M. (2018). PEDOT:PSS-based multilayer bacterial-composite films for bioelectronics. Sci. Rep. *8*, 1–12.

Zeglio, E., Rutz, A.L., Winkler, T.E., Malliaras, G.G., and Herland, A. (2019). Conjugated polymers for assessing and controlling biological functions. Adv. Mater. *31*, e1806712.

iScience, Volume *24*

Supplemental Information

Diurnal *in vivo* xylem sap glucose and sucrose monitoring using implantable organic electrochemical transistor sensors

Chiara Diacci, Tayebeh Abedi, Jee Woong Lee, Erik O. Gabrielsson, Magnus Berggren, Daniel T. Simon, Totte Niittylä, and Eleni Stavrinidou

Supplemental Information

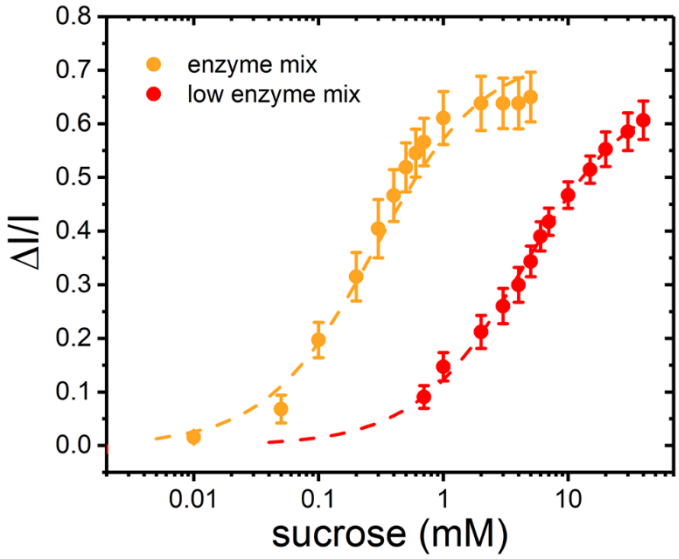

Figure S1: Calibration curves of sucrose sensors with different dynamic range in PBS buffer (Related to Figure 2)**.** Normalized response of sucrose sensors optimized for sucrose detection from 10µM to 1mM (orange) and from 1mM to 40mM (red). Dashed lines represent the sigmoid fit function. Error bars represent the standard error, n=8 for orange curve and n=5 for red curve.

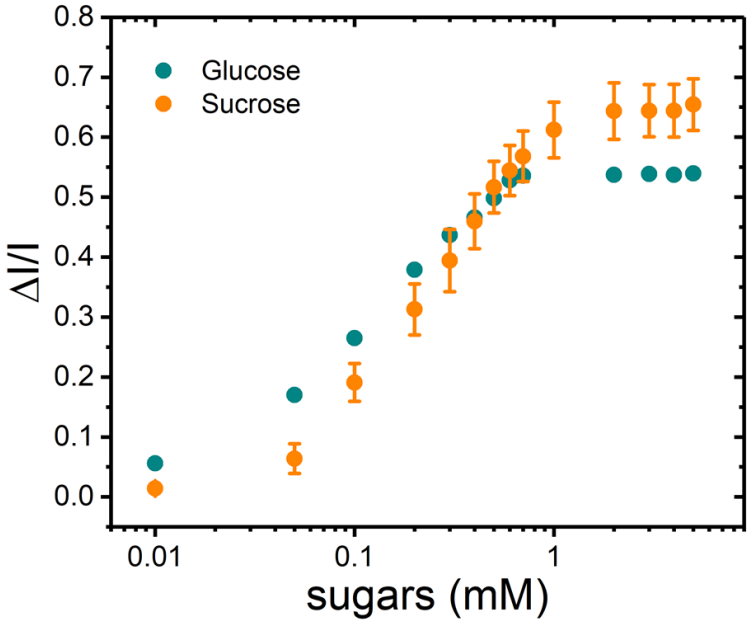

Figure S2: **Calibration curves of sucrose sensor for sucrose (orange) and glucose (cyan) solutions** (Related to Figure 2)**.** Device responses are the same for glucose solution and sucrose solution due to the presence of same amount of glucose oxidase.

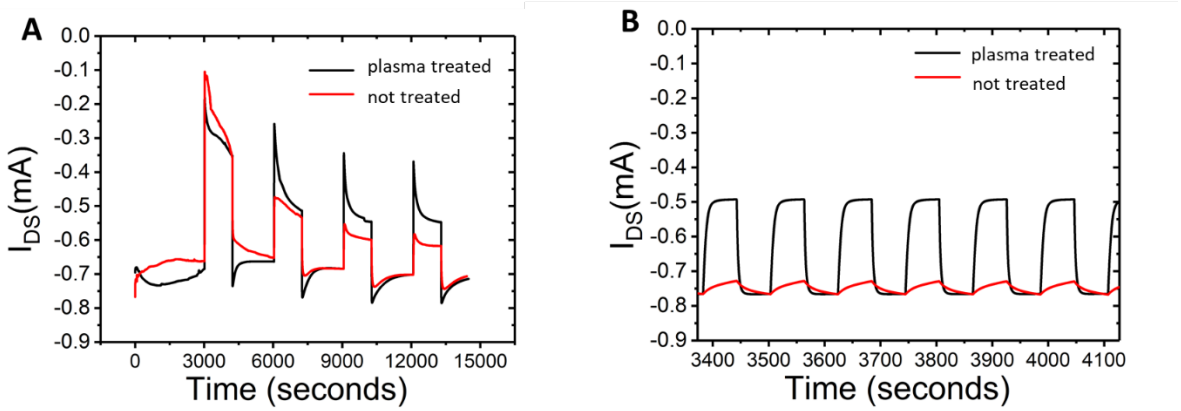

Figure S3: OECT sucrose sensors drain current I_{DS} response in the xylem tissue and effect of hydrophilicity (Related to Figure 5)**.** (A) A pulse gate voltage was applied (V_{GS} = (0V, +0.5V), V_{SD} = −0.4 V) right after insertion in the xylem tissue in device that was treated with oxygen plasma (black) and non-treated device (red). (B) Same characterization as in (a) performed after 24h from the insertion time. The non-treated device shows poor modulation.

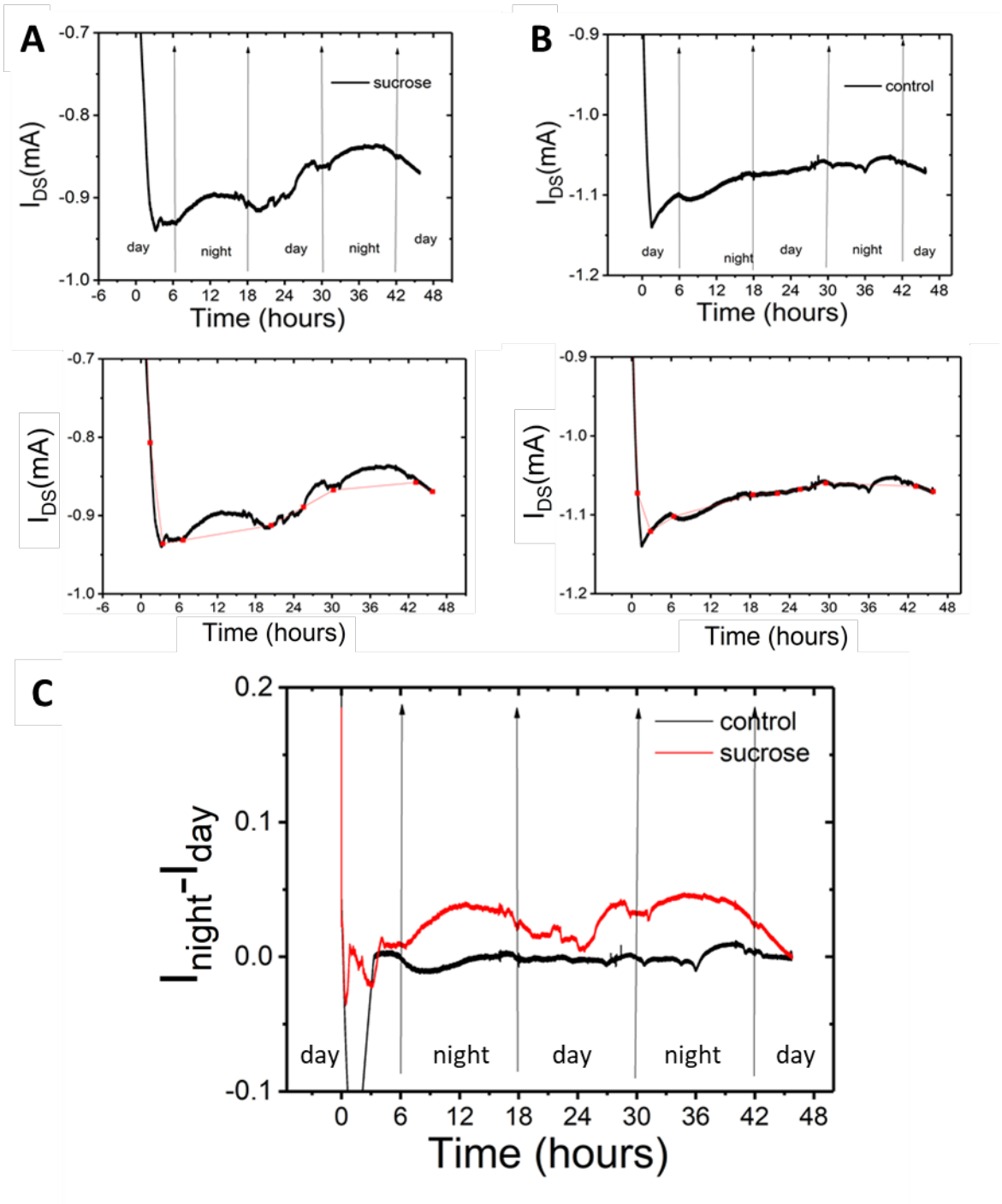

Figure S4: Baseline correction for in-vivo sensing measurements (Related to Figure 5)**.** The drain current of sucrose sensor (A) and control device (B) was recorded for 48 hours in the xylem tissue. The baseline for both measurements was defined as the drain current values during day-time, I_{day}. (C) Corrected current temporal response (I_{night}-I_{day}) for 48 hours for sucrose sensor and control device.

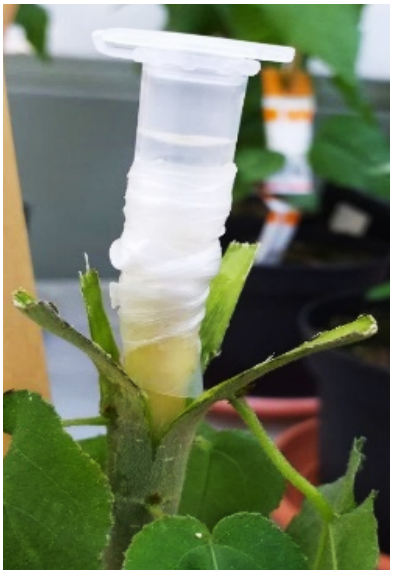

Figure S5: Xylem sap root pressure exudate collection from aspen stem (Related to Figure 5)**.**

Table S1: Soluble sugar concentrations during day as determined from ex-vivo xylem sap analysis (Related to Figure 5)

Day	**mM Glucose ± SD**	**mM Fructose ±SD**	**mM Sucrose ± SD**
Sample 1	0.30± 0.01	0.34± 0.0	0.43± 0.01
Sample 2	0.05± 0.01	0.06± 0.0	0.02± 0.01
Sample 3	0.1± 0.01	0.1± 0.0	0.16± 0.0
Sample 4	0.16± 0.01	0.21± 0.0	0.34± 0.0
Sample 5	0.22± 0.01	0.25± 0.0	0.27± 0.0
Average	**0.17±0.1**	**0.19±0.11**	**0.24 ± 0.16**

Table S2: Soluble sugar concentrations during night as determined from ex-vivo xylem sap analysis (Related to Figure 5)

Night	**mM Glucose ± SD**	**mM Fructose ±SD**	**mM Sucrose ± SD**
Sample 1	3,91± 0,02	2,92± 0,03	3,86± 0,05
Sample 2	2,95± 0,04	2,01± 0,05	5,79± 0,25
Sample 3	2,76± 0,04	2,3± 0,03	3,54± 0,09
Sample 4	2,66± 0,01	1,93± 0,01	2,66± 0,08
Sample 5	1,63± 0,02	1,35± 0,01	3,18± 0,25
Average	**2.78± 0.81**	**2.1±0.57**	**3.81±1.20**

Transparent Methods

Device fabrication

For the device fabrication a polyethylene naphtalate foil (Teonex Q65HA, 125 µm, Peutz Folien GMBH) was cut in a circular 4" substrate. The substrate was cleaned with water and acetone, then vacuum backed for 90 s at 120°C. Metal films of 2nm titanium (Ti) and 50 nm gold (Au) were evaporated onto the clean surface. Photolithography (Karl Suss MA/BM 6 mask aligner) and a Shipley 1805 positive resist were used to pattern contacts, wiring, channel and gate. The substrate was then wet etched in I_2/KI solution for Au, and $H_2O_2/NH_4Cl/H_2O$ for Ti. The remaining resist was stripped with acetone. A PEDOT:PSS (Clevios PH1000) mixture with 5% v/v EG (ethylene glycol) and 1% v/v GOPS (3-Glycidyloxypropyl)trimethoxysilane) and dodecylbenzenesulfonic acid (50 µl drop per 5 ml) was spin-coated and patterned using a Shipley 1813 positive resist, then dry etched with CF_4/O_2 reactive ions, in order to create channels and gates. The remaining resist was stripped again with acetone. In the end, the substrate was encapsulated with SU-8 2010 (MicroChem) and openings on the active areas are defined by wet etching with developer mr-Dev 600 (Microresist Techonology). Chemicals were used as received from Sigma-Aldrich unless stated otherwise.

Device functionalization

Pt nanoparticles were deposited onto the PEDOT:PSS gate electrode using a solution of 5 mM H_2PtCl_6 in aqueous 50 mM H_2SO_4, through electrochemical deposition (potentiostat, BioLogic SP-200). Deposition was performed using gate as working electrode and applying a first fixed potential of +0.7 V for 10 seconds and a second fixed potential of -0.2 V for 15 seconds. Two different enzyme mixtures were prepared to functionalize respectively sucrose and glucose sensor. The sucrose sensor mixture was prepared by adding 3 mg/ml Glucose oxidase, 5mg/ml Invertase and 2.5% v/v of Mutarotase Suspension (Wako) in in Phosphate Buffer Saline (PBS,

Thermo Fisher). The glucose sensor mixture was prepared with 3mg/ml Glucose Oxidase only. Enzyme solutions were mixed with a solution of filtered chitosan 5 mg/ml in 50 mM CH_3COOH in a proportion 1:2 and 2,5% v/v of glutaraldehyde 2.5 wt% (Sigma Aldrich). Immobilization was performed by drop-casting 1.5 µl of enzyme/chitosan mixture on the gate electrode. After 30 minutes, the electrode was rinsed with deionized water to remove the remaining CH_3COOH. Chemicals were used as received from Sigma-Aldrich unless stated otherwise.

Arduino measurement units

Each unit was built using an Adafruit Feather M4 Express microcontroller (Adafruit Industries). Each OECT channel (gate and source) circuit used one analog-digital converter (ADC), one digital-analog converter (DAC), and one precision resistor (1 kOhm for source and 1 MOhm for gate). The ADCs and DACs were configured for 12-bit operation, and the sampling times for the ADCs optimized for the expected gate/source impedances (60 µs for source, 340 µs for gate). Two PIDs running on the microcontroller regulated the channel voltages (measured at the corresponding input using the ADCs) to match the setpoints by changing the corresponding output voltage (using the DACs). The PIDs iterated at about 1700 Hz, and for each iteration the resistor voltages, calculated as the difference between channel output and input voltages, were inserted into a digital 10Hz low-pass filters. Measurements were produced at 10 Hz, by transferring the mean resistor voltages over the measurement period by serial communication through a USB cable. A LabView interface was used to send commands and collect data from the three Arduino units, and to convert the resistor voltages to gate and drain currents using Ohm's law and Kirchhoff's current law.

Devices characterization and experimental set-up

Sucrose and glucose dose-curve responses were perfomed in Phosphate Buffer Saline (50 mM pH 7.4) with a Keithley 2600 series Source Meter. All measurements were carried out at room temperature and devices were operated at constant bias mode with V_{DS}= -0.4 V and the V_{GS}= +0.5 V. Devices designated for in vivo measurements were treated with oxygen plasma (Zepto W6) at 50W for 2 minutes, in order to increase surface wettability. In vivo measurements were performed with Arduino units, in the greenhouse environment for period of 24 or 48 hours in four different trees. Devices were connected to the Arduino system through ZIF connectors and inserted subsequently a 3-4 mm scalpel incision into the tree stem. A drop of sodium alginate gel (2% in PBS) was added at the epidermis exactly at the insertion site to prevent drying of the tissue. When the gel dried it formed a seal ensuring that the insertion site was no longer exposed to air.

Plant material and growing conditions

Hybrid aspens (*Populus tremula x tremuloides*) were grown in the greenhouse in a commercial soil/sand/fertilizer mixture (Yrkes Plantjord; Weibulls Horto, http://www.weibullshorto.se) at 20/15 °C (light/dark) with a 18 h light/6 h dark photoperiod and 60% relative humidity. Trees were watered every other day and they were fertilized using approximately 150 ml 1% Rika-S (N/P/K 7:1:5; Weibulls Horto) once a week after planting. 4 hybrid aspen trees (*populus tremula x tremuloide*), 8 weeks old, were then cultivated in day-neutral photoperiodic condition (12 hour light/12 hour dark) under white fluorescent light (250 μmole m-2 s-1) at room temperature with 50-60 % relative humidity. In the sensing experiments 8-16 weeks old trees were used.

Optical microscopy images

For the stem tissue analysis after sensor insertion, cross sections were prepared from OECT insertion sites located at 3mm depth from the surface of the stem as well as control trees without sensor insertion. Then the effect of was followed for 1, 2 and 5 days. A total of 12 trees were assessed, three for each time course and three for control. For each stem five stem cross-sections at 60 µm thickness were prepared using a vibratome apparatus (Leica VT 1000S). The stem sections were then stained in 0.02% (W/V) Toluidine Blue O solution. Samples were observed under a Leica DMi8 inverted optical microscope.

Data analysis

Sucrose and glucose calibration curves (Fig.2C) were calculated by normalizing the drain current I using the equation (1):

$$\Delta I/I = \frac{I_{[M]} - I_0}{I_{[M]}} \qquad (1)$$

Where $I_{[M]}$ is the drain current (I_D) at the *[M]* concentration for sucrose and glucose and I_0 is the drain current at the baseline. The calibration curve s were fitted with a sigmoid function $y = ax/(b + x)$, were a and b are constants.

The in vivo measurements (Figure 5) recorded for 24 and 48 hours were corrected for a baseline obtained using the drain current during day-time with equation (2):

$$I_{corrected} = I_{night} - I_{day} \qquad (2)$$

Where I_{night} is the current for night-time and I_{day} is the current for day-time as described in the SI (Fig. S4). The sucrose sensor trace in Fig.5A is the average of four different experiments. Normalized average variations, Fig.5B $(I_{night} - I_{day})/I_{day}$ for sucrose (n=11), glucose (n=3) and control devices (n=9) were calculated considering current values at the halftime of the measurement for day-time and night-time. For each experiment we always used a new device. For the experiments with a duration of 24 hours we get one set of data for day/night cycle. For the experiments with duration of 48hours we get 2 set of data of day/night cycle from the same device. The bar chart corresponds to the average of the normalized signal $(I_{night} - I_{day})/I_{day}$ both for the 24hours duration experiments and 48hour duration experiments.

Ex-vivo xylem sap collection and analysis

For collecting xylem sap, root pressure exudate method was used (Alexou *et al.*, 2013). Plants were cut at the bottom of trees about 10 cm from soil surface and then 1–2 cm of the bark below the cut site was removed. Then root pressure sap was collected in individual plant at midday and midnight for 1 hour (Figure S5 and Tables S1, S2).

Soluble sugars; Glucose (Glc), fructose (Fru) and sucrose (Suc), in xylem sap were assayed enzymatically (Stitt *et al*., 1989). Briefly, 50 µl of diluted xylem sap was bolide for 10 min and then was used for soluble sugar measurement. Glc, Fru and Suc contents were sequentially quantified in each sample by enzyme-based spectrophotometric assay of $NADP^+$ reduction at 340 nm.

Alexou, M. and Peuke, A. D. (2013) 'chapter 13 Methods for Xylem Sap Collection', *Plant Mineral Nutrients*, 953(July), pp. 195–207.

Stitt, M. *et al.* (1989) '[32] Metabolite levels in specific cells and subcellular compartments of plant leaves', in *Biomembranes Part U: Cellular and Subcellular Transport: Eukaryotic (Nonepithelial) Cells*. Academic Press, pp. 518–552.